A CONCEPT FOR SEEDING 4-40 nm FEL RADIATION AT FLASH2

Kirsten Hacker#, TU, Dortmund, Germany

Abstract

This note describes a scheme to seed the FLASH2 FEL over a range of 4-40 nm without impacting SASE capabilities. This scheme combines multiple seeding techniques, builds on current infrastructure and offers a maximized range of performance with higher pulse energies than what are available at lower-peak current facilities. The concept relies on Echo Enabled Harmonic Generation (EEHG), cascaded seeding, and Second Harmonic Afterburners (SHAB) while maintaining the possibility to operate with High Gain Harmonic Generation (HGHG) seeding at >30 nm wavelengths.

INTRODUCTION

High Gain Harmonic Generation (HGHG) and an HGHG cascade have demonstrated seeding at FERMI down to 19 nm with HGHG alone and 4 nm in an HGHG cascaded configuration [1,2]. FERMI operates with low-charge, 400-600 A peak current and weak compression. They have a laser heater and no space for a long, SASE undulator. All of these conditions are the opposite of those presently available at FLASH. In order for FLASH2 to offer a competitive seeding program to users while maintaining SASE capability

- the facility must be compatible with SASE
- first few years of operation without a laser heater
- seeding should work at short, 4 nm wavelengths
- seeding should work over the entire bunch-train
- design must be flexible in order to accommodate different electron beam conditions.

To fulfill these criteria, the seeding methods used at FLASH2 should be High Gain Harmonic Generation (HGHG) down to 40 nm, Echo-Enabled Harmonic Generation (EEHG) down to 7 nm, and an EEHG cascade down to 4 nm and below. Any of these seeding methods can be used with a Second Harmonic After-Burner (SHAB) to reach shorter wavelengths [3]. An HGHG cascade could be attempted, but the tolerances are not generous.

Simulations will show the limitations of each of these radiation (CSR), and laser pulse distortions using 1-D tracking and analytic estimates for 3-D effects. The full-bunch simulation methods from [4] would be used in a final design study.

Each of the seeding concepts, excluding the afterburner, could be tested in FLASH1 in 2014 [5, 6]. The hardware required for these tests has already been commissioned and experts are available for the operation.

Through the FLASH2 configuration shown in Fig. 1, individual commissioning of HGHG, EEHG and an EEHG cascade could be accomplished in a stepwise fashion, allowing for work starting with proven concepts at 40 nm and ending with seeding at 4 nm. 2 nm could potentially be seeded given an afterburner [3]. HHG could also be incorporated into the setup in an EEHG-HHG configuration, but this concept is an add-on of research interest for compact schemes and it is not essential to the design for user operation.

An item which is essential for seeding is the Transverse Deflector Structure (TDS) drawn at the end of the FEL radiator. Aside from providing an unparalleled diagnostic of the overlap of the seed with the electron bunch, this X-band longitudinal beam diagnostic would be shared with the LAOLA plasma wakefield acceleration experiment in FLASH3 [7] and provide information on the FEL pulse length to users.

This paper includes brief descriptions of

- electron beam and laser parameter ranges
- TDS design and resolution
- chicane, modulator and laser injection design
- impacts of electron bunch compression schemes
- impacts of laser parameters
- a simulation of HGHG and EEHG
- the conditions for EEHG cascade and SHAB

The conclusion is that by building a flexible, staged design which has the potential to seed the shortest possible wavelengths for the maximum 1.3 GeV FLASH electron beam energy, a competitive program can be developed for FLASH2 to deliver the benefits of external seeding to the FEL users in terms of longitudinal coherence, increased intensity, direct control over pulse properties and spectral stability.

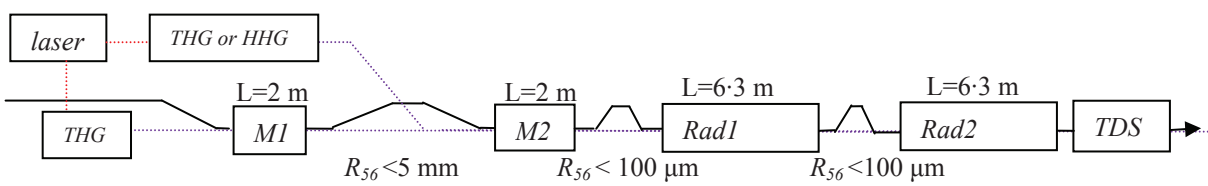

Figure 1: A flexible design for FLASH2 allowing for SASE, HGHG, EEHG, EEHG-HHG, HHG and an EEHG cascade, facilitating seeding between 4 and 40 nm. Harmonics of the Ti:sapphire laser pulse can be generated through Third Harmonic Generation (THG) or High Harmonic Generation (HHG). Two modulators (M1, M2) could be used to facilitate a flexible seeding program, while a Transverse Deflecting Structure (TDS) could diagnose the longitudinal profile and energy spread of the electron beam.

#*kirsten.hacker@cfel.de

ISBN 978-3-95450-133-5

ELECTRON BUNCH

The electron bunch can be compressed and shaped in many different ways. An example of a reasonable electron bunch for seeding is shown with images from a measurement done by C. Behrens using a Transverse Deflector Structure (TDS) to streak out the electron bunch longitudinally (Fig. 2) [8]. The basic constraints of the electron bunch parameter space for seeding are given in Table 1.

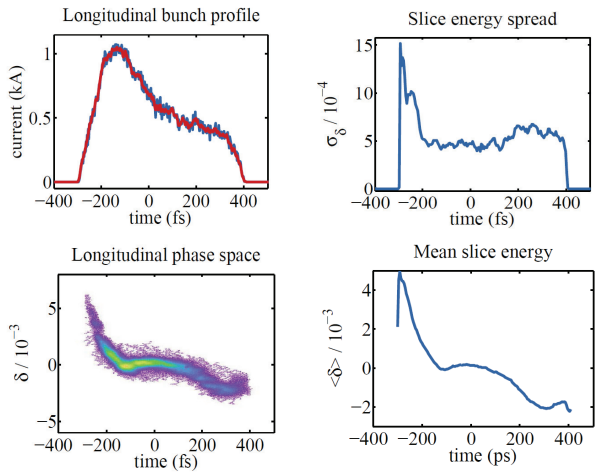

Figure 2: Measured slice energy spread (left), and deviation of the slice energy from the nominal (right). At 1 GeV and with 1 kA. From C. Behrens [8].

Table 1: Electron Bunch Parameters for Seeding

Electron bunch for seeding	
Bunch length	~50 μm (rms)
Energy	<1.3 GeV
Emittance	1.5 mm mrad
Peak current	1-2 kA
Slice energy spread (rms)	100-500 keV

Looking at the electron beam in Fig. 2, one sees that the properties are not uniform along the bunch and that only a small fraction will have the high peak current and low slice energy spread for seeding to be successful. While an uncorrelated energy spread of 50 keV can be simulated for the FLASH2 beamline, such performance has never been observed in FLASH1.

Since the portion of the bunch which has the appropriate properties for seeding is only ~50 fs (rms) (Fig. 2), the synchronization with the ~20 fs (rms) duration of an external laser pulse necessitates the 25 fs (rms) performance of the intra-bunch train feedback and optical synchronization system [9]. It also requires an accurate diagnostic of the longitudinal overlap between seed and electron bunch. This is why a TDS diagnostic installed after the radiator is needed for a successful seeding program.

A TDS streaks the electron bunch out longitudinally so that when it is impinged upon a screen, the charge density as a function of longitudinal position is depicted. After a dispersive section, the energy spread of the electron bunch is given as a function of the longitudinal position along the bunch. When such a diagnostic is installed after a radiator, the increase in the energy spread of the electron bunch is indicative of energy loss due to radiation of photons in the FEL process. By comparing FEL-on to FEL-off images, one can use the measurement of the energy lost during radiation as a measurement of the longitudinal profile of the FEL light pulse. This has been done at SLAC with a 2 meter long X-band TDS which has gotten 4 fs (rms) resolution with a 13 GeV beam and a 25 MW klystron [10].

A similar cavity, with a smaller, L6145 6 MW klystron, could be used to generate comparable performance with FLASH's 1.3 GeV beam. It could be installed in a 3 meter long section after the last SASE undulator in FLASH II and it would be useful for

- giving users information about the longitudinal profile of the FEL pulse for each bunch train
- R&D for LAOLA ultra-short bunch diagnostics
- commissioning the FLASH II extraction line
- operating any seeding experiments

The slice energy spread increases caused by a seed can be observed on the longitudinal phase space of the electron bunch and allow for optimization of the overlap. While this would be useful for HGHG, it would be indispensable for EEHG because it clearly facilitates the longitudinal overlap of two seed pulses with the seedable portion of the electron bunch.

For a beam energy of 1 GeV, a frequency of 9.3 GHz, and a normalized emittance of 1.5 μm (rms), the temporal resolution of an X-band TDS in FLASH II would be

$$\tau[\mathrm{fs}] = 474/(V[\mathrm{MV}]\cdot\sqrt{\beta[\mathrm{m}]}\cdot\sin(\vartheta))$$

where V is the deflection voltage, β is the beta function at the deflector and ϑ is the phase advance between the deflector and the screen. For example, for V= 20 MV, β = 16 m, $\vartheta=\pi/2$, then 6 fs (rms) resolution should be expected. For FLASH3 (LAOLA) [7], a larger beta function could be used with their smaller emittance in order to approach the sub-fs resolution which they require. For FLASH2, the smaller, 16 m beta function is needed in order to avoid impacting more than two SASE undulators with a large β and in order to maintain a 90 degree phase advance to the dump screen.

The 2 meter long X-band cavity is only marginally more compact than a 2.856 GHz S-band cavity, but due to the shorter wavelength, it offers 3 times the streaking strength so that a weaker klystron can be used. Instead of a 20 MW S-band klystron with a 2.44 meter long LOLA structure, a 6 MW X-band klystron could be used with a 2 m long 9.3 GHz structure to generate 20 MV of streaking voltage. By adding a pulse compressor to the 6 MW klystron, 12 MW would be available to the cavity, further improving the resolution. By sharing the FLASH2 klystron and modulator with the plasma wakefield experiment in FLASH3 and collaborating with XFEL and

ISBN 978-3-95450-133-5

other groups on the LLRF development, efficiencies could be exploited.

SEED LASER

The OPCPA seed laser system for FLASH2 produces pulse trains of tunable 740-800 nm with 1 mJ per pulse in the train. These pulses can be compressed to 30-40 fs (FWHM) [11]. The seed pulse trains are designed to seed every 10th bunch in the electron bunch train. The laser can also be operated in single-pulse (10Hz) operation, without pulse trains but with more energy per pulse (Table 2). Another option is to send the 500 mJ 800 nm laser from the plasma wakefield experiment into the FLASH2 tunnel. This laser would provide more power than is required for HGHG or EEHG, but it could be used to produce a powerful HHG beam for seeding.

Table 2: IR Laser Parameters for Generating a UV Seed

IR laser options	Pulse-train (100 kHz)	Single-pulse (10Hz)
Wavelength (nm)	740-800	740-800
Peak power (GW)	1.75	30
Pulse energy (mJ)	1	20
FWHM duration (fs)	40	40

The ~800 nm pulses from these different laser configurations can be converted into ~270 nm through frequency multiplication in BBO crystals or they can be frequency multiplied through HHG in a gas jet to make much shorter wavelengths with dramatically reduced conversion efficiency. The frequency multiplied pulses could be injected in either the last bend of the dogleg or in the first EEHG chicane as seeds for the electron bunch.

The 270 nm seed for the first modulator would be injected after the last vertical bend of the extraction line, 11 meters prior to the modulator. There is enough offset at the bend for a 25 mm mirror to inject a beam with a maximum size of 9 mm FWHM on the mirror. The seed for the second and third modulators could be injected in the first chicane where space for an injection mirror is not limited. The injection point in the chicane could be used to deliver the 270 nm seed to the second modulator, located upstream of the first radiator section. It would be compatible with HHG injection but this is only a research option and not central to the concept.

Since a minimum 1:3 ratio in the diameter of the electron beam compared to the seed beam is desirable to avoid degradation of the bunching from the non-uniformity of the transverse laser intensity profile [12], the minimum seed waist which would be desirable for a 50-100 μm (rms) electron bunch would be 350-800 μm (FWHM).

The optimal electron bunch waist is determined by the type of modulator which is used. A short modulator with four 0.1 m long periods could be used with a small electron beam size if the primary goal is to seed with the shortest possible pulses. Such a modulator would minimize the slippage, but it would not make the most efficient use of a limited amount of laser power and it would not smear out unwanted correlated phase errors in the seed pulse [13]. A longer modulator of 2 meters with 30 periods would allow for a more efficient use of the seed laser power and it is the preferred modulator in this design. The laser parameters for this modulator are in Table 3.

Correlated longitudinal phase errors or chirp do not directly shorten the portion of the seeded beam which will radiate in the FEL as was claimed [14,15]. Instead, the slippage in the modulator averages out the error and makes it possible to seed nearly transform limited FEL pulses [13]. The correlated phase error (α) does, however increase the peak field requirement of the seed (E_0) according to a calculation of the energy modulation along the bunch where $p(t)$ is the position of the seed with respect to the electron beam, k is the wavenumber, σ_s, is the seed pulse length, and L_m is the length of the modulator [13],

$$\gamma_m(s) = \int_0^{L_m/c} \frac{e}{m_e c^2} E_0 e^{-[s-p(t)]^2/4\sigma_s^2} e^{i\{k[s-p(t)]+\alpha[s-p(t)]^2+\phi\}} \cdot v_x(t) dt$$

Table 3: Seed Parameters in Modulators for Seed Generated through THG in BBO Crystals

THG seed for EEHG/HGHG modulators	
Seed wavelength	250-270 nm
Peak power	<175 MW
Pulse energy	<100 μJ
FWHM pulse duration	40 fs
Seed waists	350-800 μm (FWHM)
Electron beam waist	50-100 μm (rms)

To analytically describe the influence of a distorted seed wavefront in the second undulator on the EEHG bunching factor, one can calculate the bunching factor suppression as a function of distortions of the 270 nm seed (λ_s) [4],

$$\frac{b_{error}}{b_{noerror}} = e^{-2\pi^2 a^2 \left(\frac{\sigma_{\lambda_s}}{\lambda_s}\right)^2} \quad (1)$$

where a is the harmonic number. The suppression factor for a range of harmonics of 270 nm and wavefront distortions is plotted in Fig. 3.

CHICANE DESIGN

The first chicane, responsible for folding the beam in EEHG, should be made as long and gentle as space allows with the shortest possible dipoles. Since it would also be used to do a fraction of the final compression of the electron bunch, the beam size should be smallest at the last dipole in the plane of deflection [16]. Given the current FLASH2 lattice with 3.3 m between quadrupoles in a FODO cell, a chicane length of 3 m would fit, however, given the planned 350 mm long dipoles, this

ISBN 978-3-95450-133-5

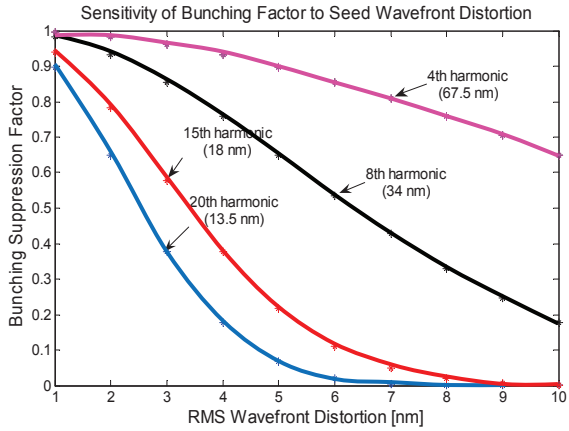

Figure 3: The bunching suppression factor for a range of harmonics and wavefront distortions.

would not leave enough space for incoupling a seed and one would need to build a second chicane for that purpose. The alternative is to turn a 6.6 m FODO cell with two chicanes into just a FO containing one longer chicane with 300 mm long HERA dipoles. The longer chicane reduces the energy spread increase due to CSR in the folding and incoupling chicane by an amount described by the worst-case, steady-state estimates in Table 4 below.

Table 4: Worst-Case CSR Energy Loss for a Gaussian Bunch with 50 μm (rms) Length and 1.2 kA of Peak Current in the EEHG Folding and Injection Chicane in the case that the 6.6 m FODO cell is preserved with two short chicanes or if it is converted into a 6.6 m FO cell with 3 meters between the dipoles

Dispersion	FODO chicanes	FO chicane
1 mm	2 MeV	0.8 MeV
5 mm	2.9 MeV	1.4 MeV
10 mm	3.5 MeV	1.7 MeV

The energy loss due to CSR from the macrobunch is not a big problem for seeding because, while it is non-linear, the seed is very short relative to the scale of the nonlinearities, so the seeded portion experiences this macrobunch CSR as a change in linear energy chirp.

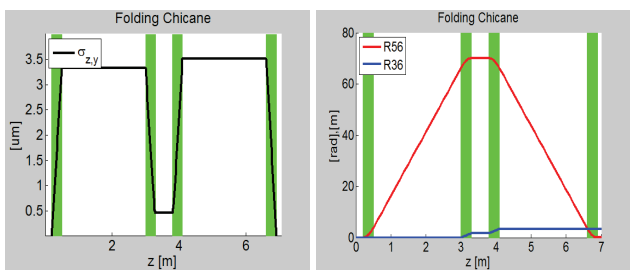

Figure 4: Transverse smearing of charge due to tilt as a function of longitudinal position in folding chicane. Green boxes represent magnet locations. Peak current is highest between the first two dipoles, ruling out danger of microbunch CSR.

The CSR for the seeded microbunch is a different problem. As long as the high peak currents in the EEHG folding process only occur in the first chicane in regions with significant transverse smearing (z,y tilt), disastrous CSR effects in the first chicane can be avoided. To check this, the location of maximum compression was calculated and compared to the smearing plotted in Fig. 4.

The largest effect of micro-bunch CSR arises at the exit of the chicane which is used to do the final bunching as shown with the CSR wake [17] in Fig. 5. This is, however, an over-estimate of the wake, since the full compression is not reached until the last fraction of the dipole and there is significant transverse smearing at the entrance to the dipole which is not included in the calculation. If the final compression is accomplished through the velocity bunching of a 30 m drift, then CSR can be avoided completely.

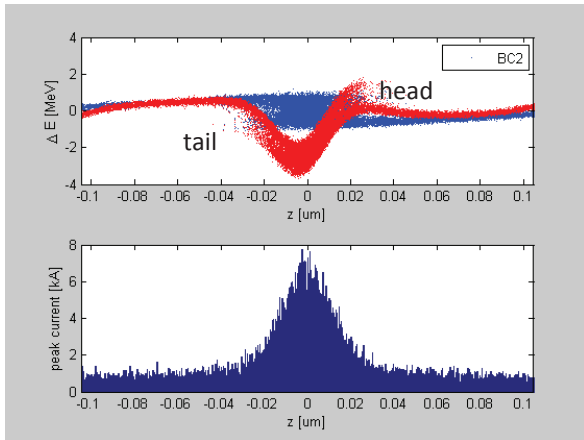

Figure 5: An HGHG microbunch (blue) under the influence of a worst-case steady-state CSR wake (red) in a 100 mm long dipole. The head of the bunch is to the right.

Table 5: Folding and Bunching Chicane Parameters

First chicane at 1GeV	
Pole Gap	40 mm
Magnetic field	280 mT
Physical length	300 mm
Magnetic length	360 mm
Deflection angle	<30 mrad
Dist. btw. dipoles	3 m
Dispersion (R_{56})	<2.7 mm
Max current	3.5 A
Vacuum chamber	100 mm
Second and third chicanes at 1GeV	
Pole Gap	40 mm
Magnetic field	300 mT
Physical length	100 mm
Deflection angle	9 mrad
Dist. btw. dipoles	0.75 m
Dispersion (R_{56})	130 μm
Max current	3.5 A
Vacuum chamber radius	17 mm

ISBN 978-3-95450-133-5

The parameters of the chicanes are in Table 5. The first chicane uses HERA magnets fitted with 40 mm pole shoes and the second chicane uses FLASH correctors.

LONGITUDINAL SPACE CHARGE

Incoming density modulations are transformed into an energy modulation ($\Delta\gamma$) in the presence of impedance (Z) [17].

$$\Delta\gamma = \frac{|Z(k)|}{Z_0}\frac{I_0}{I_A}\rho_i \qquad (2)$$

where Z_0 = 377 Ω is the impedance of free-space, I_A = 17 kA is the Alfen current, and ρ_i is a small current perturbation at some wavenumber k. This energy modulation is transformed into bunching in a dispersive section. CSR, Longitudinal Space Charge (LSC), geometric wakes, and Coherent Edge Radiation (CER) all contribute. Together they accumulate to create the Micro-Bunching Instability (MBI). The largest contribution by far is made by LSC because it accumulates along the entire machine. The other effects are stronger, but they accumulate over shorter distances.

While FLASH does not have a laser heater to reduce the LSC induced microbunching instability, a special setup of the machine can potentially reduce the microbunching gain by orders of magnitude compared to its manifestation for a typical SASE setup of the machine. By using the 1 ps short-pulse injector laser instead of the 6.4 ps SASE injector laser, one can avoid using the first bunch compressor. Although the energy spread will be more non-linear, the peak current will be smaller through the following acceleration stages, thereby reducing the growth of the microbunching instability. A simulation of a FLASH-like machine done in [18] showed that the microbunching gain with single-stage compression is an order of magnitude smaller than with two-stage compression. The start-to-end simulations done in [4] are consistent with this strategy.

Aside from setup of the accelerator and bunch compressors, the setup of the seeding section undulators and chicanes has an impact on the MBI. For example, if a fully compressed microbunch is transported over 4 meters, the energy chirp reverses and the peak current is reduced (Fig. 6). If, however, the seeded microbunches are transported in an undercompressed state over a few meters, the LSC wake has a beneficial effect: it acts to reduce the energy spread of the microbunch [19-21]. If the length L of the drift is too long or the LSC potential is too strong, then the microbunches will be destroyed. An optimal condition is achieved when the the $R_{56}=L/\gamma^2$ velocity bunching dominates.

There are significant differences between the shape and magnitude of LSC wakes for EEHG microbunches and HGHG microbunches as shown in Fig. 7 for $kr_b<\gamma/2$,

$$Z_{LSC}(k) = \frac{iZ_0}{\pi k r_b^2}\left[1 - \frac{kr_b}{\gamma}K\left(\frac{kr_b}{\gamma}\right)\right] \qquad (3)$$

where $r_b=0.85(\sigma_x+\sigma_y)$ is the radius of a uniform, round beam with radius 100 μm, K is a modified Bessel function, and γ is the Lorentz factor [22] . Note that when the microbunch becomes shorter than the transverse size of the beam, as in the EEHG case, the LSC potential assumes the form of an error function. The potentials from neighboring microbunches cancel each other out except for on the ends. This means that for EEHG, each burst of microbunches will have distortions on the ends and for HGHG and EEHG there will be distortions due to the Gaussian profile of the seed. Imperfect cancellation of these potentials in the tails could lead to shorter than expected seeded FEL pulses.

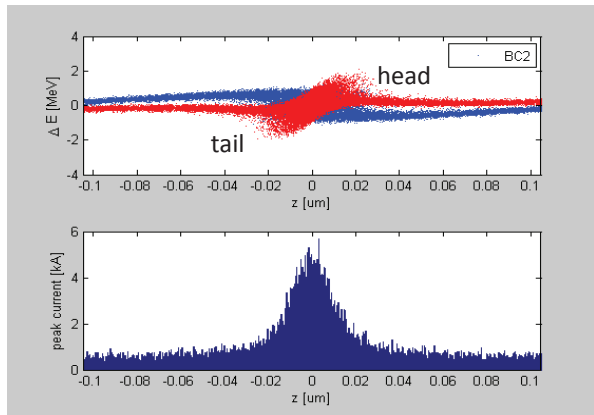

Figure 6: The effect of the LSC potential on a 100 μm (rms) radius HGHG microbunch transported by 4 meters. Blue is the unaffected distribution and red includes the LSC wake.

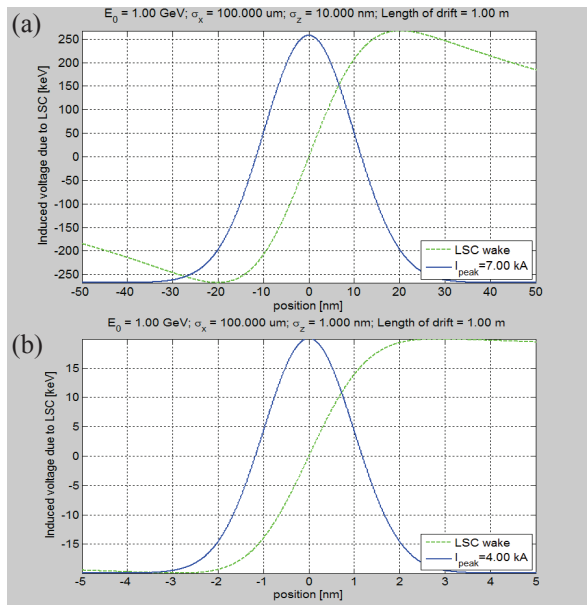

Figure 7: LSC wake per meter for (a.) HGHG microbunch with length of 10 nm (rms) and peak current of 7 kA and (b.) EEHG microbunch with a length of 1 nm (rms) and peak current of 4 kA. The beam radius is 100 μm (rms). The rms length excludes particles surrounding the microbunch and that wakes of neighboring microbunches impact the tails but not the slope of the wake.

ISBN 978-3-95450-133-5

HGHG OPERATION

HGHG was proposed in 1980 [23] and it relies on energy modulation of the electron bunch produced through interaction with a seed laser in an undulator tuned to the seed wavelength. Microbunches with the periodicity of the seed laser are then produced through the energy dependent path length differences in a chicane (Figs. 8, 9). The radiator undulator is tuned to a seed harmonic.

HGHG can be used as a low-risk first attempt at seeding in FLASH2. It can also be done with the high repetition rate configuration of the seed laser with an ample overhead in the laser power budget. The 1 mJ, 40 fs 800 nm laser pulses can be converted into 100 µJ, 40 fs 270 nm seed laser pulses through frequency tripling in BBO crystals giving a maximum of 175 MW. This seed would be injected in the first chicane in the seeding section and it would be used to seed in the second modulator (M2) with a waist of 700 µm (FWHM) over 30 periods. The energy modulation would be 2 MeV (peak-to-peak) with a 40 MW peak power seed out of an available 175 MW. Above this amount of energy modulation, the gain of the FEL decreases. A 50 µm R_{56} bunches the modulated beam and the beam energy is 700 MeV.

A complication arises with transporting a bunched beam to the radiator undulators at the end of the machine. In the absence of LSC, one should expect $R_{56} = L/\gamma^2 = 15$ µm of dispersion over the L=26 meters from the exit of the modulator to the entrance to the last radiator segment (Rad2) and the net R_{56} required to bunch the beam for 2 MeV energy modulation is ~50 µm. One can use the chicane between the two radiator sections to do the final bunching so that the distance that the bunched beam travels to the radiator is minimized. A small, beneficial reduction in the energy spread of the microbunch is facilitated through the LSC potential in the drift when the beam radius is ~200 µm (rms), but if the beam radius is smaller, then LSC destroys the bunching [19-21].

By taking the Fourier transform of the longitudinal charge density distribution (Fig. 9), the bunching factor as a function of harmonics of the seed wavelength can be calculated for a range of initial slice energy spreads (Fig 10). Since a 1.5 kA beam with a bunching factor of <0.06 (represented by the purple line) will not reach saturation in less than four U32 undulator segments [5], one can use Fig. 10 to make a prediction of the minimum wavelength which can be seeded with HGHG at FLASH2. When CSR and LSC are taken into account, they will suppress the bunching factor for smaller energy spreads. Figure 10 does not take this into account. It can be compared with Fig. 2 of [4] in which a larger energy modulation was used.

Using 150 keV as a reasonable prediction of the likely energy spread for a 1.5 kA electron bunch [4], 38.5 nm could be seeded at FLASH II with a 270 nm seed. Since the 800 nm laser is tunable down to 740 nm, one could extrapolate that the tripled beam would have a wavelength of 247 nm and it could seed down to 35 nm. If two additional U32 undulators are used as an SHAB, the seeded wavelength could be divided by two.

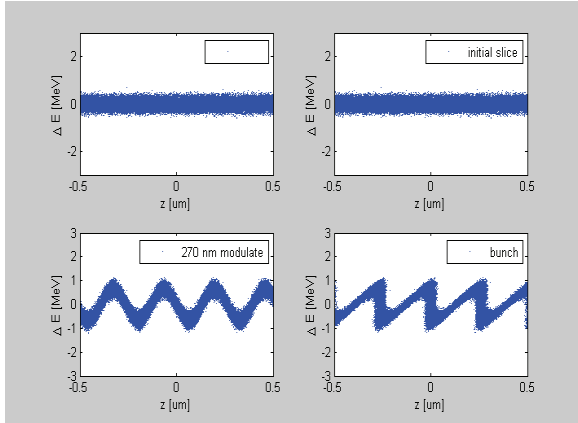

Figure 8: Longitudinal phase space of slice of electron bunch before and after energy modulation with external seed and bunching in a magnetic chicane. A seed with 40 MW of 270 nm and a 700 µm (FWHM) diameter was used with an electron beam with 150 keV (rms) initial slice energy spread.

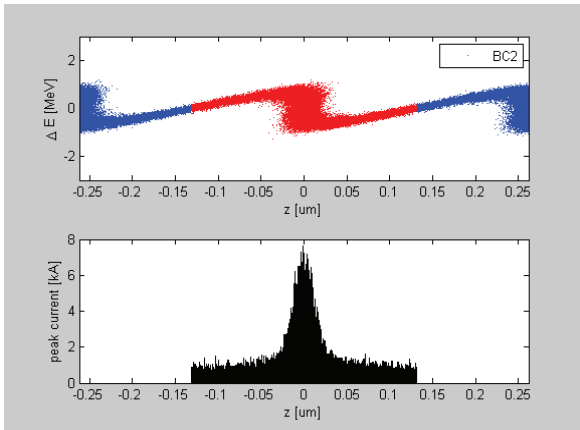

Figure 9: Projection of electrons in longitudinal phase space is used to calculate the peak current of the microbunches for a 1.5 kA initial peak current beam.

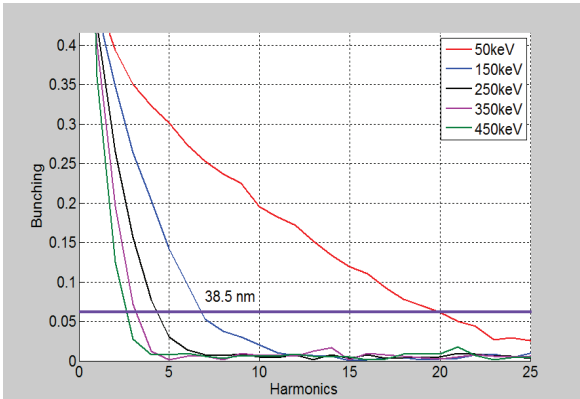

Figure 10: Bunching factor for HGHG with different initial slice energy spreads. The minimum wavelength

ISBN 978-3-95450-133-5

which can be seeded with 270 nm and a 150 keV energy spread is 38.5 nm.

EEHG OPERATION

EEHG was proposed in 2008 to overcome the limitations of HGHG in terms of electron beam energy spread tolerances and harmonic number [12]. It calls for the co-propagation of an electron bunch and laser pulse through an -undulator, chicane, undulator, chicane- series. Through interaction with a seed laser, the electron beam develops an energy modulation in an undulator which is then over-compressed in a chicane, creating horizontal bands of charge with discrete energies. The electron bunch is then modulated again in a second undulator and compressed in a second chicane, resulting in vertical stripes of charge with a period consistent with a harmonic of the seed laser wavelength. It has so far been demonstrated by SLAC in the NLCTA facility at the 14th harmonic of the seed [24, 25] and at the DUV-FEL at SINAP [26].

One could seed the entire bunch train with 1 mJ, 40 fs (FWHM) of 800 nm converted into 100 μJ of 270 nm (175 MW). Splitting the seed laser pulses transversely into two beams with ~50 μJ in each seed, one injects the seeds at two locations: the dogleg and the first EEHG chicane. This would allow one to use smaller, 500 μm (FWHM) waists in both 2 meter long modulators. With such conditions, one could achieve the bunching shown in Figs. 11-13 with 20 MW in each modulator, out of an available 175 MW. The dispersion for folding and compression was 1 mm in the first chicane and 60 μm in the second chicane.

It is important to have a laser power overhead because if the laser pulse has a chirp, the energy modulation will be smaller than for the transform limited pulses which were used in these simulations [13]. 20 meter drifts of the energy modulated yet unbunched beam are also dangerous in the presence of LSC. If a large, 200 μm beam radius is not enough to remove the LSC problem in the 20 m drift, the modulated beam should be bunched immediately after the modulator and sent directly into the radiator. If the radiator is too far from the user extraction, then a split-radiator scheme should be used.

In 2010, SINAP did start-to-end simulations of EEHG for FLASH2 [27] and the configuration shown here is, in large part, similar to the SINAP configuration. Their investigations done through GENESIS and CSR Track are still valid. They predicted seeding down to 7 nm through EEHG with 1.2 GW of 270 nm focused to 700 um (FWHM). The electron beam energy was 700 MeV and the R_{56} =1 mm in the folding chicane. They also predicted seeding at 4 nm using the same laser conditions, but with a 1.22 GeV beam energy and a 5.5 mm R_{56} in the folding chicane, but the tolerance of CSR and other distortions becomes more difficult than at 7 nm.

A study of EEHG tolerances for FLASH1 was done in [5]. It tolerates electron beam and laser pulse intensity jitter well. Compared to HGHG it tolerates a very large slice energy spread, but the trade-off is tight tolerances on the magnetic fields leading up to the radiator.

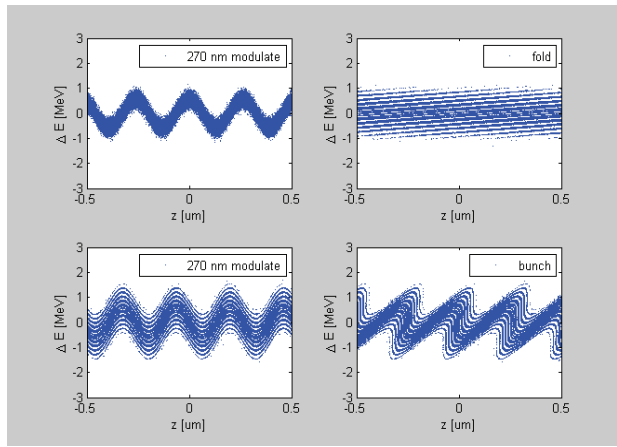

Figure 11: Folding and bunching in longitudinal phase space using a 20 MW 270 nm seed with a 700 um (FWHM) waist. 150 keV is the initial slice energy spread.

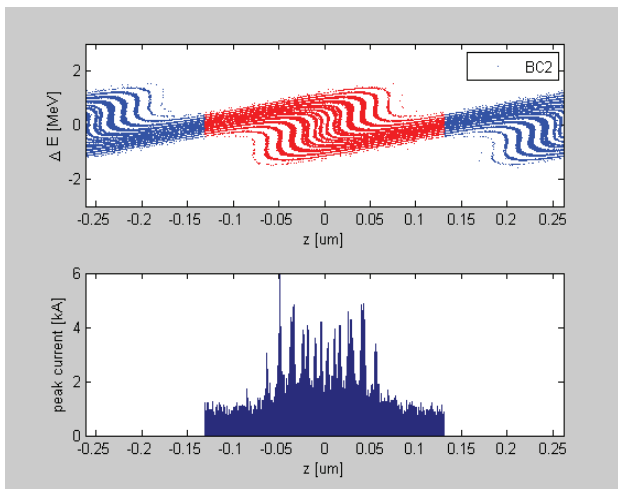

Figure 12: Projection of electrons in longitudinal phase space is used to calculate the peak current of the microbunches.

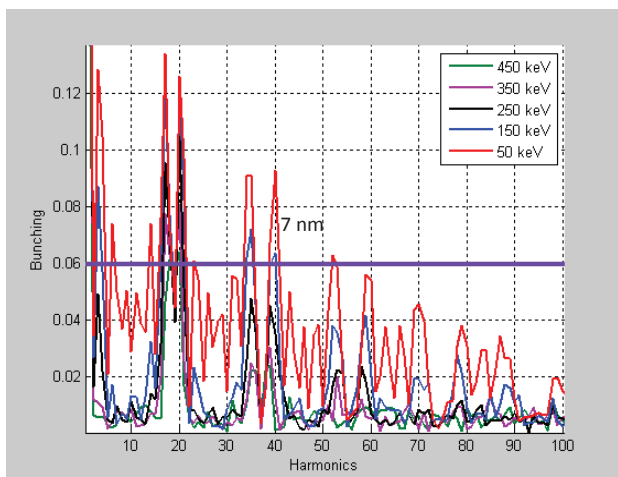

Figure 13: Bunching factor for EEHG with different initial slice energy spreads. The minimum wavelength which can be seeded with 270 nm and a reasonable, 150 keV energy spread is 7 nm.

ISBN 978-3-95450-133-5

EEHG-HHG OPERATION

EEHG-HHG (Figs 14-16) uses an HHG beam to seed in the second EEHG stage. It uses the same layout as regular EEHG, but it is more suitable for seeding on the few-nm scale. It was briefly proposed in 2011 for SWISS-FEL seeding at 1 nm, but it was rejected in favor of self-seeding due to concerns about synchronization and risk [28]. The biggest concern about such a scheme at FLASH is the intensity and quality of the HHG seed pulse required to generate the 250 keV to 500 keV of energy modulation necessary for this scheme to work. A peak power of 250-500 kW with a waist of 350 μm (FWHM) in a 2 meter long undulator with 30 periods is required by this scheme. For a 30 fs pulse length, the pulse energy would need to be 15 nJ.

This would not be a first-line method to attempt seeding at 4 nm. The EEHG cascade would have looser tolerances for the seed, but EEHG-HHG is interesting research because of its potential for use in compact FEL designs. The HHG mechanism in a gas is fundamentally different from the THG which occurs in a BBO crystal and one can imagine potential advantages in terms of the seed wavefront quality of an HHG pulse compared to a THG pulse.

With a loosely focused, phase matched HHG arrangement at sFLASH, 30 fs long 20 mJ pulses of 800 nm were used to produce up to 35 nJ of 38.1 nm with $M_x^2 = 9.5 \pm 3.1$, and $M_y^2 = 4.4 \pm 2.7$. After 95% losses in transport and 75% losses through overlap, only a fraction of a nanojoule was coupled into the electron beam [29,30]. This is consistent with other literature and optimized coupling of the seed energy into the electron beam, but it is a confusing contrast with literature describing 10 μJ produced at 73.6 nm, 4.7 μJ at 62 nm, 1 μJ at 54 nm, 330 nJ at 29.6 nm and 25 nJ at 13 nm with a 30 fs 16 mJ wavefront shaped IR beam [31,32]. These higher conversion efficiencies are representative of the energy scaling of HHG for different wavelengths, but they were achieved through looser focusing than what sFLASH can use. sFLASH has to use a smaller focus so that the focal spot in the undulator will be matched to the electron bunch. Two-mirror telescopes with direct incidence of XUV light cannot be used because they have unacceptable losses. Capillaries and phase matched cells do not come into consideration because they don't work well for wavelengths longer than 20 nm.

By putting a loosely focused source adjacent to the FLASH II injection, and injecting it with a pair of grazing incidence mirrors, minimal losses can be expected compared to the 95% losses in sFLASH transport, but the 800 nm laser for FLASH II has 95% less peak power than the sFLASH laser, making the expectation of an improvement in the HHG seed power at 38.5 nm compared to sFLASH unrealistic. However, by using 60 nm or 70 nm instead of 38.1 nm, one might expect 10-20 times more conversion efficiency for an expected output of 30-60 nJ for a 1 mJ input pulse. This would be 2-4 times the 15 nJ EEHG-HHG requirement.

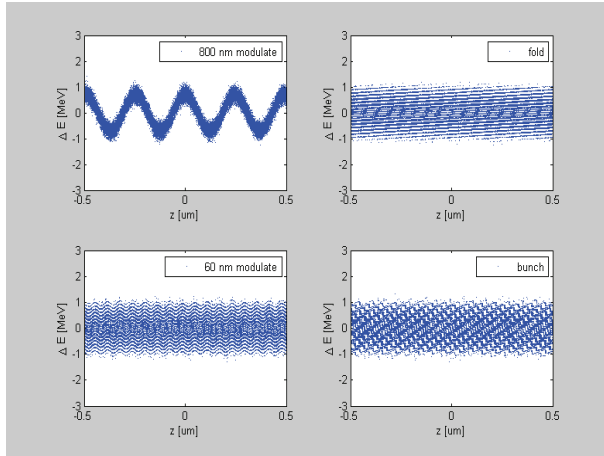

Figure 14: Folding and bunching in longitudinal phase space using a 40 MW 246 nm seed with a 700 μm (FWHM) waist and a 500 kW 61.6 nm seed with a 350 μm (FWHM) waist. 150 keV is the initial slice energy spread.

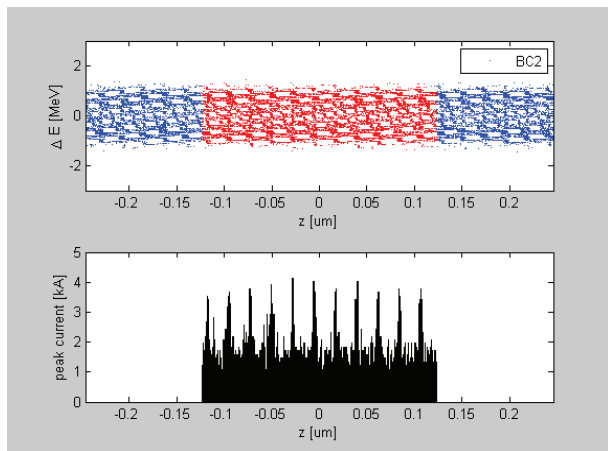

Figure 15: Projection of electrons in longitudinal phase space is used to calculate the peak current of the microbunches.

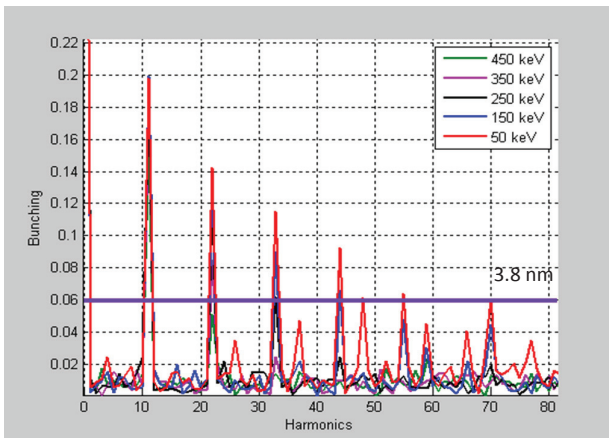

Figure 16: Bunching factor for EEHG with different initial slice energy spreads. The minimum wavelength which can be seeded with 270 nm and a 150 keV energy spread is 7 nm.

ISBN 978-3-95450-133-5

CASCADED OPERATION

A major benefit of a cascade is the wavefront quality that the seed in the second stage gains by saturating in the first radiator stage. This makes it possible to reach shorter wavelengths with a cascade than are possible through a single-stage seeding scheme which is limited by the seed laser quality (Fig. 3).

The idea behind a fresh-bunch cascade technique is that the portion of the bunch which was seeded in the first radiator (Rad1) is too heated to be used to radiate in a second undulator stage (Rad2), so the radiation from the first stage must be positioned over a fresh, un-modulated portion of the bunch in the second stage [33]. The challenge of the technique is to overlap the radiation from the tail of the bunch with an appropriate portion of the head of the bunch by using a small chicane to delay the electron bunch relative to the light.

An HGHG fresh-bunch cascade has been used at FERMI to seed 4 nm [2] but a similar, three-stage cascade cannot fit into FLASH unless SASE operation is sacrificed, due to space constraints. Another critical difference is that the FERMI cascade is not separated from the linac by a dogleg, as is the case for FLASH2. Coupled with the lack of a laser heater at FLASH, even with the low-charge, weak compression scheme used at FERMI, identical performance should not be expected.

A two-stage, fresh-bunch cascade (Fig. 1) can, however, be used in FLASH2. When used with an HGHG seed, it would be limited to a minimum of 10 nm (the 3rd harmonic of 30 nm) and it would require a small, 150 keV (rms) slice energy spread. An EEHG cascade could, however, tolerate a large, 450 keV (rms) slice energy spread and seed 4 nm (the 3rd harmonic of 12 nm). This tolerance makes an EEHG cascade more suitable for a SASE machine setup and it could facilitate a seeded beam with a higher charge and therefore higher output power than what can be accomplished through a low-charge FERMI-like design.

For a two-stage, fresh-bunch cascade to work, the radiation intensity from the first radiator stage (Rad. 1) must be sufficient to seed in the second radiator stage (Rad. 2). Based on GENESIS simulations [4], the radiated 14 nm beam size at the exit of 3 U32 undulators after reaching saturation would be ~100 μm (rms) and the divergence would be ~20 μrad (rms). The peak power for a 1.5 kA electron bunch would be 1 GW. The 3rd harmonic of 14 nm would have a smaller divergence and power. One can derive an expression for a harmonic's power from the spectral density per electron of the radiation emitted in the forward direction for the m^{th} harmonic [34],

$$\frac{d^2U_m}{d\Omega d\omega} = \frac{e^2\gamma^2 m^2 K^2}{4\pi}\cdot\frac{\sin^2\left(\pi N_u(\omega-\omega_m)/\omega_1\right)}{\sin^2\left(\pi(\omega-\omega_m)/\omega_1\right)}\cdot|JJ|^2$$

where

$$JJ = J_n\left(\frac{mK^2}{4+2K^2}\right) - J_{n+1}\left(\frac{mK^2}{4+2K^2}\right),\ m=2n+1.$$

The radiated power for a given harmonic is proportional to the spectral energy [31],

$$U_m(\omega) = \frac{d^2U_m}{d\Omega d\omega}\Delta\Omega_m \qquad (4)$$

contained in the solid angle $\Delta\Omega_m=2\pi\sigma_{\theta,m}$. If one plots U_m as a function of radiated wavelength for 3 U32 undulators with K=2.66, one sees that the 3rd harmonic has about half of the spectral energy of the fundamental radiation within the solid angle defined by Eq. 4 (Fig. 17).

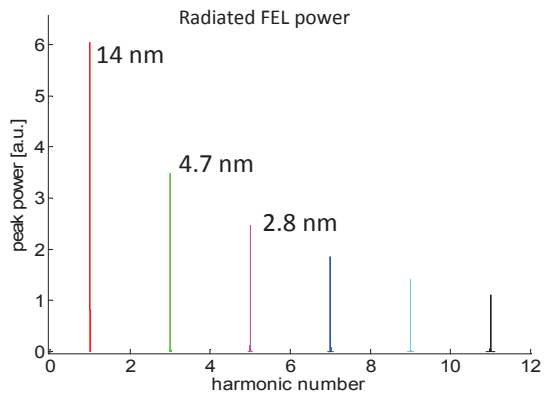

Figure 17: The radiated power of the m^{th} harmonic emitted into the solid angle $\Delta\Omega_m$. The Lorentz factor γ = 2250, the undulator period λ_u = 3.14 cm, and the K parameter is 2.66.

Based on Fig. 17, one would expect the 3rd harmonic to have half of the 1 GW peak power of the fundamental for a 1.5 kA electron beam and 1/3 of the ~30 μrad (rms) divergence. If the peak intensity coming directly out of the first radiator stage is then 1.1 GW/cm^2, 20 meters downstream, it would have an intensity of 0.25 GW/cm^2.

1 GW/cm^2 for seeding at ~5 nm is the seed intensity required to suppress fluctuations of the higher harmonics and it is several orders of magnitude higher than the intensity required to merely establish temporal coherence [35]. From this criteria, one could conclude that if EEHG seeding at <20 nm is successful in the first radiator stage (Rad1), fresh-bunch cascading in the second radiator section (Rad2) is possible with a significant safety margin. To suppress fluctuations of the higher harmonics in order to incorporate a <4 nm afterburner, the distance between the two radiator stages would need to be minimized.

The conditions described above could be achieved in an EEHG cascade starting with 10-20 nm in the first stage. For an HGHG cascade, the wavelength in the first radiator would be longer (30-40 nm) and the divergence and beam size would be about a factor of 2 larger, reducing the intensity in the second radiator stage compared to the

ISBN 978-3-95450-133-5

EEHG cascade, but the intensity threshold for establishing temporal coherence is about 0.5 GW/cm^2 lower for the longer wavelengths used in an HGHG cascade.

In conclusion, an EEHG or HGHG cascade could work at the 3rd harmonic. An EEHG cascade is a much more robust option in terms of slice energy spread tolerance compared to an HGHG cascade, however, the tolerance of magnetic field errors in the first-stage of EEHG seeding is tighter than for HGHG.

SUMMARY OF OPERATION MODES

Several different operation modes were outlined in the preceding sections. Each mode has a different tolerance of the initial slice energy spread of the electron beam. Plots summarizing the ranges of operation for a best-case 150 keV slice energy spread are drawn below (Fig. 18). The EEHG options offer more robust performance under poor, 450 keV slice energy spreads.

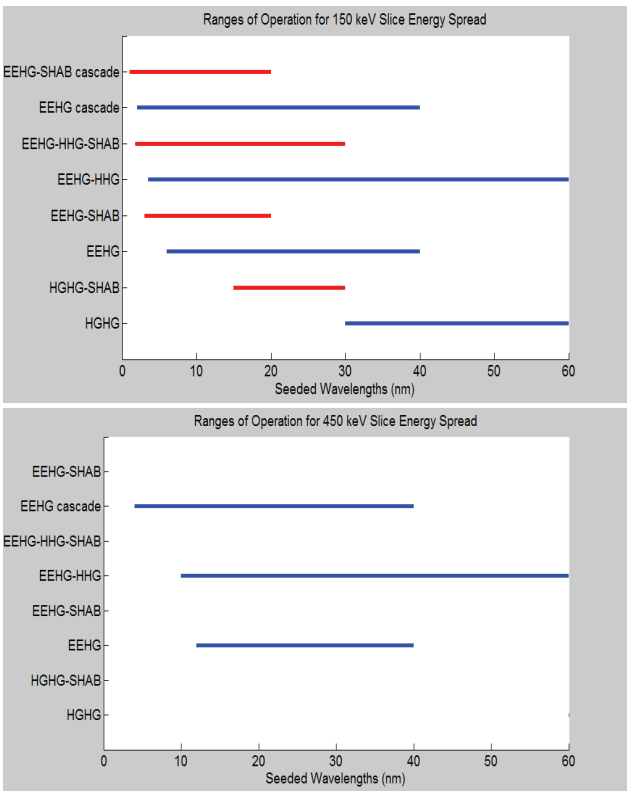

Figure 18: Summary of minimum wavelengths for different types of seeding configurations for the best-case 150 keV (rms) uncorrelated energy spread which has been measured at FLASH and for a poor, 450 keV (rms) uncorrelated energy spread.

CONCLUSION

The concept outlined in this note would allow for a conservative startup at FLASH2 using HGHG with parallel progress towards sub-4 nm seeding using EEHG techniques. All of the concepts illustrated here can be first tested in FLASH1 in 2014, allowing for design work to conclude in 2015 and purchase to proceed in 2016. Prior to seeding purchases, TDS purchases should commence as soon as possible, for installation in 2015, so that the diagnostic will be available for extraction line commissioning.

ACKNOWLEDGEMENTS

Thank you to Bart Faatz for information on the FLASH II layout and plans and to Joerg Rossbach and Shaukat Khan for reviewing the document.

REFERENCES

[1] E. Allaria, et al., Nat. Photon. 6, 699 (2012).
[2] E. Allaria, et al., Nat. Photon. 7, 913 (2013).
[3] V. Vardaanyan, et al., TESLA-FEL-2012-03.
[4] G. Feng, et al., These Proceedings: Proc. 36th Int. Free-Electron Laser Conf., Basel, 2014, MOP083.
[5] K. Hacker, H. Schlarb TESLA-FEL-2011-04.
[6] K. Hacker, et al., TESLA-FEL-2011-05.
[7] http://laola.desy.de/
[8] C. Behrens, DESY-THESIS-2012-03.
[9] I. Grguras et al., Nat. Photon. 6, 852–857 (2012).
[10] C. Behrens et al.,. Nat. Comm. 5, 3762 (2014).
[11] T. Tanikawa et al., These Proceedings: Proc. 36th Int. Free-Electron Laser Conf., Basel, 2014, MOP081.
[12] D. Xiang and G. Stupakov, SLAC-PUB-13644, 2009.
[13] C. Feng, et al., Phys. Rev. ST Accel. Beams 16, 060705 (2013).
[14] D. Ratner, et al., Phys. Rev. STAB 15, 030702(2012).
[15] G. Geloni, et al., arXiv: 1111.1615v1.
[16] E.L. Saldin, E.A. Schneidmiller, and M.V. Yurkov, TESLA-FEL 1997-08.
[17] E.L. Saldin, E.A. Schneidmiller, and M.V. Yurkov, TESLA-FEL 1996-14.
[18] R.A. Bosch, K.J. Kleman, and J. Wu, Phys. Rev. STAB 11, 090702 (2008).
[19] K. Hacker, FLASH seminar 2013 (Nov, 12 2013).
[20] K. Hacker, DESY Reports, TESLA-FEL 2013-01.
[21] K. Hacker, These Proceedings: Proc. 36th Int. Free-Electron Laser Conf., Basel, 2014, MOP095.
[22] Z. Huang, et al., Phys. Rev. STAB 7, 074401 (2004).
[23] I. Boscolo, V. Stago, Nuovo Cimento B 58 (1980) 267.
[24] E. Ferrari, et al., Proc. 35th Int. Free-Electron Laser Conf. Manhattan, 2013, THOANO03.
[25] D. Xiang et al., Proc. 35th Int. Free-Electron Laser Conf. Manhattan, 2013, THOANO02.
[26] H. Deng et al., Nature Photonics 6, 360 (2012).
[27] H. Deng, et al., DESY Report, DESY-11-034.
[28] E. Prat et al., Proc. 33rd Int. Free-Electron Laser Conf. Shanghai, 2011.
[29] Th. Maltezopoulos et al., Appl. Phys. B, doi: 10.1007/s00340-013-5571-6 (2013).
[30] S. Ackermann et al., Phys. Rev. Lett. 111 114801 (2013).
[31] E. Takahashi et al., Phys. Rev. Lett. A, 66 021802(R) (2002).
[32] E. Takahashi et al., Appl. Phys. Lett., Vol. 84, Num. 1, (2004).

ISBN 978-3-95450-133-5

[33] I. Ben-Zvi, K.M. Lang, L.H. Yu, Nucl. Instrum. and Meth. A 318, p. 726 (1992).
[34] P. Schmueser, et al., "Ultraviolet and Soft X-Ray Free-Electron Lasers," Springer p.14-16 (2008).
[35] L. Giannessi, Proc. of FEL 2004 Trieste, Italy.

ISBN 978-3-95450-133-5